
01 Nov 1982

Elastic Differential Cross Sections for Small-Angle Scattering of 25-, 50-, and 100-keV Protons by Helium Atoms

Jerry Peacher

Missouri University of Science and Technology, peacher@mst.edu

Thomas J. Kvale

E. Redd

Paul J. Martin

et. al. For a complete list of authors, see https://scholarsmine.mst.edu/phys_facwork/1354

Follow this and additional works at: https://scholarsmine.mst.edu/phys_facwork

 Part of the [Physics Commons](#)

Recommended Citation

J. Peacher et al., "Elastic Differential Cross Sections for Small-Angle Scattering of 25-, 50-, and 100-keV Protons by Helium Atoms," *Physical Review A*, vol. 26, no. 5, pp. 2476-2481, American Physical Society (APS), Nov 1982.

The definitive version is available at <https://doi.org/10.1103/PhysRevA.26.2476>

This Article - Journal is brought to you for free and open access by Scholars' Mine. It has been accepted for inclusion in Physics Faculty Research & Creative Works by an authorized administrator of Scholars' Mine. This work is protected by U. S. Copyright Law. Unauthorized use including reproduction for redistribution requires the permission of the copyright holder. For more information, please contact scholarsmine@mst.edu.

Elastic differential cross sections for small-angle scattering of 25-, 50-, and 100-keV protons by helium atoms

J. L. Peacher, T. J. Kvale, E. Redd, P. J. Martin,* D. M. Blankenship, E. Rille, V. C. Sutcliffe,[†] and J. T. Park

Physics Department, University of Missouri, Rolla, Missouri 65401

(Received 20 April 1982)

The first measurements of elastic differential cross sections have been carried out for 25-, 50-, and 100-keV protons scattered through very small angles by helium atoms. The University of Missouri—Rolla energy-loss spectrometer provided the required high angular resolution and also separated the elastically scattered ions from the inelastically scattered ions. The data are compared to our Born, Glauber, and classical calculations as well as a four-state calculation. All of the measured elastic differential cross sections are more sharply peaked than theory for the smallest scattering angles. At the larger scattering angles all of the measured elastic differential cross sections are below the theoretical calculations. However, if the classical calculation is interpreted as a total differential scattering cross section, it compares well with our estimate of the sum of the elastic, charge-transfer, and inelastic differential cross sections.

INTRODUCTION

The measurement of the elastic scattering cross section for 25- to 100-keV protons scattered from helium atoms is complicated by the necessity to distinguish the elastically scattered ions both from the inelastically scattered ions and from the unscattered ions. The University of Missouri—Rolla (UMR) differential ion energy-loss spectrometer¹ provides the needed high resolution in both energy loss and scattering angle. The high resolution in energy loss permits positive identification of inelastically scattered ions. The high angular resolution permits measurements at very small scattering angles. Therefore, the UMR differential ion energy-loss spectrometer is the ideal apparatus for studying elastic scattering.

This measurement is the first published report of an elastic differential cross section in the intermediate impact energy range. There have been several previous measurements of total scattering cross sections in the keV ion impact energy range.²⁻⁶ These measurements did not result in a genuine elastic differential cross section because the inelastic and elastic scatterings could not be adequately separated. All experiments including the one reported here suffer from an inability to distinguish elastically scattered ions from the transmitted unscattered ions near zero scattering angle.

The present measurements are of elastic differential cross sections for proton-helium scattering at

very small angles. The angular resolution is 120 μ rad (0.007°). The total angular range of the experiment is from 0.5 to 3.0 mrad (0.172°) in the center-of-mass frame which is less than the angular resolution of the previous total scattering cross-section measurements in the keV energy range. The negative aspect of the high angular resolution is a low count rate which rapidly decreases with increasing scattering angle. It is this factor which limits the angular range of the experiment. The positive aspect of the high resolution is that the measurements provide differential cross sections covering an angular scattering region which has been previously unaccessible.

Similarly there are surprisingly few theoretical calculations of elastic differential cross sections in this energy range. Most of the available theoretical calculations use classical approaches which are expected to be invalid for very small angle scattering.⁷⁻¹⁶ Included in this paper are our calculations of the elastic differential cross section using Born, Glauber, and classical approximations with the static potential. The four-state results of Flannery and McCann¹⁷ are also compared with our measurements.

EXPERIMENTAL METHOD

The differential ion energy-loss spectrometer and the general method employed have been discussed

in detail elsewhere^{1,18-21} in connection with the measurement of inelastic differential cross sections. The experimental method employed in the present experiment only differs from the method employed to measure inelastic cross sections in that there is no inelastic energy loss. The elastically scattered ion beam is unambiguously distinguished from the inelastically scattered beam by the energy resolution of the energy-loss spectrometer.

The apparatus is a linear accelerator-decelerator system. The accelerator section includes the ion source, extraction lens, velocity filter, beam focusing, steering, and profile monitoring elements. The decelerator contains the energy analysis and beam detection apparatus. The collision region and mass analyzer are located between the accelerator and decelerator sections. The accelerator section and collision region are rotated as a unit about an axis that passes through the collision point, allowing the measurement of cross sections which are differential in both scattering angle and energy loss.

In a collision of an ion and a target atom, the scattered ion loses energy due to the recoil of the target atom even if no inelastic process is involved. The recoil energy loss is calculated and set by the controlling minicomputer for each measurement. The measurement scattering angle, count time, target pressure, and transmitted ion current are controlled and/or monitored by the minicomputer which simultaneously corrects the measurements for scattering chamber pressure deviations, instrument and residual gas caused background, and normal incident beam drift.

The angular distributions of the incident and elastically scattered beams are measured by recording the transmitted ion current while pivoting the apparatus about the scattering center. The incident beam's angular distribution and all corresponding background current distributions measured in this manner comprise a sequence of angular data.

Data were taken using two different target chambers. Initially data were taken with the existing target chamber while a second target chamber whose scattering interaction length could be accurately determined was being designed and built. The existing target chamber was designed using exit and entrance cones. This arrangement minimized scattering from defining aperture edges. However it prevented an accurate measurement of the scattering interaction length which is needed in order to determine an absolute differential cross section. The second target chamber was designed both to eliminate scattering from defining apertures and to

permit an accurate determination of the interaction length. The pressure in this chamber was measured by both an MKS Baratron 170 and an older Baratron 77. The pressure was maintained constant during a measurement by a microcomputer-based pressure controller using the analog signal from the MKS Baratron 170.

Absolute differential cross sections were calculated using the techniques discussed below for the second chamber when both the target gas pressure and the interaction length were accurately measured. Relative data from the chamber whose interaction length was uncertain were normalized to the absolute differential cross sections using a single normalizing constant. The statistical errors shown as error bars on the graphs were calculated using all the data.

The "zero energy-loss" current I detected at the analyzer is the sum of the transmitted and elastically scattered ion beams. Analysis of the scattering process²¹ provides a rate equation for the detected ion current which has not suffered any inelastic energy loss. This equation which includes second-order processes is given by

$$\frac{dI}{d(nl)}(\theta) = \int_{\Delta\Omega} d\Omega' \int d\Omega \frac{dI}{d\Omega}(\hat{k}) \frac{d\sigma_e}{d\Omega'}(\hat{k}' \cdot \hat{k}) - I(\theta)\sigma_T, \quad (1)$$

where \hat{k} is a unit vector in the direction of the incident ion, \hat{k}' is a unit vector in the direction of the scattered ion, $d\sigma_e/d\Omega'$ is the elastic differential cross section, $\Delta\Omega$ is the solid angle subtended by the detector, and σ_T is the total cross section for all processes: elastic, charge transfer, and inelastic. The angle θ is the angle between the accelerator axis and a line from the center of the collision region to the center of the detector. The integration over $d\Omega$ is over all incident ion directions and the integration over $d\Omega'$ is over all scattered ion directions that are seen by the detector. This deceptively simple equation is the fortuitous result of the cancellation of several terms which appear in its derivation. Equation (1) is actually a series of coupled equations at various angles θ . The series of equations can be solved by expanding $I(\theta)$ as a function of nl ; namely,

$$I(\theta) = I_0(\theta) + nlB_1(\theta) + (nl)^2B_2(\theta) + \dots,$$

where $I_0(\theta)$ is the incident ion beam current. To lowest order in nl this approach yields

$$\int_{\Delta\Omega} d\Omega' \int d\Omega \frac{dI_0}{d\Omega}(\hat{k}) \frac{d\sigma_e}{d\Omega'}(\hat{k}' \cdot \hat{k}) = I_0(\theta)\sigma_T + B_1(\theta). \quad (2)$$

The terms I_0 , B_1 , B_2 , etc., can be determined from transmitted ion beam measurements taken at various pressures. Measurements were also taken from pressure sweeps at fixed angles. To first order, $B_1 = (I - I_0)/nl$.

At angles which exceed the angle where the incident beam distribution falls to zero [$I_0(\theta) = 0$], Eq. (2) can be solved using the same technique employed in the determination of inelastic cross sections. At smaller angles B_1 is negative and $-B_1 \cong I_0\sigma_T$. For very small angles,

$$(I_0\sigma_T + B_1) \ll |B_1|.$$

At zero angle the statistical noise in the data would need to be reduced to less than 0.2% to obtain reliable values for $I_0\sigma_T + B_1$. For this reason the cross sections are not reliable for angles where $I_0\sigma_T + B_1$ is less than the uncertainty in B_1 ; however, an estimate of $I_0\sigma_T + B_1$ is needed for all angles in order to use the unfolding technique.¹ Because $B_1(\theta) \cong -\sigma_T I_0$ at very small angles, σ_T can be estimated from the data. At these very small angles this estimated value of σ_T is used with the measured values of $B_1(\theta)$ to fit the data to a second-order polynomial in θ . The value for $\Delta\sigma_e/\Delta\Omega$ at zero angle obtained as a result is used to correct the original estimate of σ_T and the fitting process is repeated.

The elastic differential cross section $d\sigma_e/d\Omega$ is extracted from Eq. (2) using techniques developed for the calculation of inelastic cross sections.¹ The data-analysis method relates the convolution integral in Eq. (2) to the elastic differential cross section $d\sigma_e/d\Omega$. The analytical representation of the convolution integral involves an integration of $d\sigma_e/d\Omega$ over the measured incident beam distribution and the solid angle subtended by the detection window. The numerical method employed extracts $d\sigma_e/d\Omega$ by equating the measured values of $B_1(\theta) + I_0(\theta)\sigma_T$ to its integral representation at each acquisition angle. The process is described in detail in Ref. 1.

THEORY

Various theoretical calculations were carried out for comparison with the experimental results. The Born approximation, the Glauber approximation,

and the classical approximation were all calculated using the static potential field of the target helium atom. Cox and Bonham²² expressed the static potential as a sum of screened Coulomb potentials and used a least-squares method to fit this analytical form to the potential obtained from Hartree-Fock wave functions calculated by Clementi and Roetti²³ for helium. The various theoretical calculations were simplified considerably by using this analytical form of the static potential.

Both the Born and Glauber approximations²⁴ are straightforward if the static potential is represented by a sum of screened Coulomb potentials. The Born scattering amplitude is obtained in analytical form. The Glauber scattering amplitude is reduced to an integral over the impact parameter. This integral was carried out numerically using standard techniques. The elastic differential cross section for each approximation is given by the absolute value of the appropriate amplitude squared.

The classical approximation⁹ for small-angle scattering was also carried out. In this approximation straight-line trajectories are assumed and the transverse momentum is related to the impulse during the collision. This approximation yields a scattering angle which is a function of the impact parameter for a given straight-line trajectory. The elastic differential cross section is then calculated in the usual manner.

RESULTS

The measured elastic differential cross sections are shown in Figs. 1–3. The error bars shown represent only the rms statistical errors. Possible systematic errors resulting primarily from the calibration and analysis technique are not included.

The possible sources of systematic error are minimized by the measurement technique. The incident current is measured immediately before and after the measurement of the scattered ion current and because the analysis uses the ratio of these currents, this possible source of error is small in the present measurement. The uncertainty in the pressure was less than 5%. The interaction length and the solid angle subtended by the detector were known to within 1%. However, the effects of error in the solid angle are minimized by the data-analysis technique.¹ The data-analysis technique itself is, of course, a potential source of error. While the analysis of the data is very complex at very small angles, the same analysis has minimal effect at the larger scattering angles reported. At angles greater than 1 mrad in the center-of-mass system, the elas-

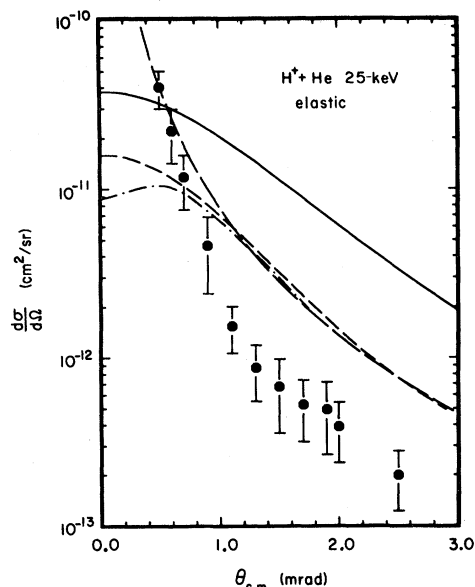


FIG. 1. Elastic differential cross section for proton-helium scattering in the center-of-mass frame for a proton with a laboratory energy of 25 keV. ●, present data; —, Born calculation; ---, Glauber calculation; —·—, classical calculation; ·····, four-state calculation of Flannery and McCann (Ref. 17). The error bars indicate random errors only. Systematic errors are discussed in the text.

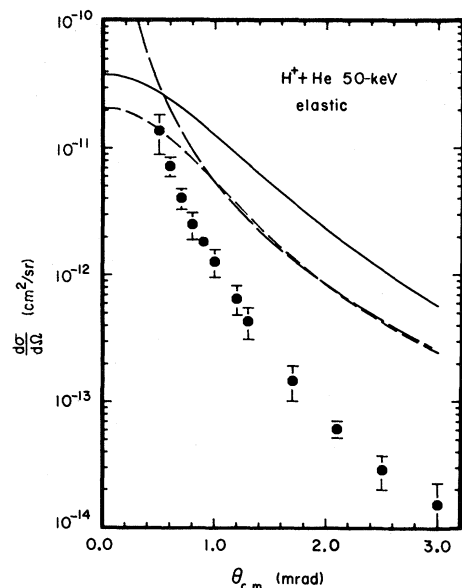


FIG. 2. Elastic differential cross section for proton-helium scattering in the center-of-mass frame for a proton with a laboratory energy of 50 keV. ●, present data; —, Born calculation; ---, Glauber calculation; —·—, classical calculation. The error bars indicate random errors only. Systematic errors are discussed in the text.

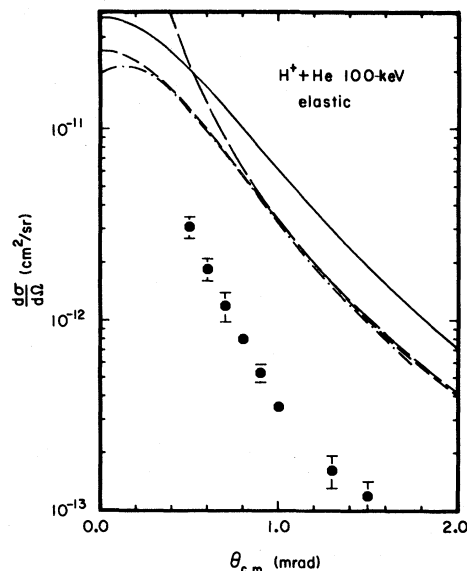


FIG. 3. Elastic differential cross section for proton-helium scattering in the center-of-mass frame for a proton with a laboratory energy of 100 keV. ●, present data; —, Born calculation; ---, Glauber calculation; —·—, classical calculation; ·····, four-state calculation of Flannery and McCann (Ref. 17). The error bars indicate random errors only. Systematic errors are discussed in the text.

tic differential cross section is very nearly¹ $\Delta\sigma_e/\Delta\Omega = I/(I_t n l \Delta\Omega)$, where I_t is the total current of the elastically scattered beam. The use of I_t in place of the total incident beam current corrects the measurements for beam loss due to charge-changing collisions.¹⁸ Comparisons of this "apparent" differential cross section with the output of the analysis program indicate that the analysis program is not contributing any significant systematic errors. Systematic errors other than those arising from the data-analysis technique would tend to affect the magnitude of the cross section but have little effect on the curve shape.

Our calculated elastic differential cross sections are also shown in Figs. 1–3. Our Born approximation result is essentially identical to the Born approximation calculation reported by Flannery and McCann.¹⁷ All of the calculations except the Born become very similar to the classical calculation at larger scattering angles.

DISCUSSION

Direct comparison with earlier work is not meaningful both because the earlier measurements could not isolate the elastic scattering and because the an-

gular resolution of the present measurement is so much better than the earlier measurements. The Fitzwilson and Thomas⁶ measurement of $d\sigma/d\Omega$ for elastic plus inelastic scattering (excluding charge transfer) of 20-keV protons by helium reaches 5×10^{-15} cm²/sr at their smallest scattering angle of 10 mrad in the center-of-mass frame. This compares to 2.0×10^{-13} cm²/sr at our largest angle of 2.5 mrad at 25 keV. The scattering measurements of Fitzwilson and Thomas⁶ and of Crandall, McKnight, and Jaecks² are in general agreement with classical scattering theory.⁷ However, at the smallest angles covered in their experiments, the experimental cross-section curves are noticeably below the classical theoretical curves. This trend is consistent with the observed differences between the theoretical calculations and the present experiment.

A possible source of the discrepancy between the theoretical and our experimental results is the failure of the theoretical treatments to adequately account for the effects of the various inelastic channels; particularly ionization and charge-transfer. The agreement between theory and experiment is fairly good for total differential scattering cross-section measurements^{2,6} which include the inelastic channels. This suggests that theoretical treatments do not completely isolate the elastic channel from the inelastic channels.

Measurements previously reported from this laboratory can be used to obtain a rough estimate of the total differential scattering cross section. The UMR differential ion energy-loss spectrometer has been employed to measure the differential cross section for excitation of helium to the $n=2$ singlet level by proton impact¹ and for charge-transfer to all states in the proton-helium collision.²⁵ The excitation differential cross section can be used to estimate a total excitation differential cross section by using the n^{-3} scaling rule.²⁶ While it is recognized that ionization and excitation differential cross sections are unlikely to have the same angular dependence, the excitation differential cross section can

$$\begin{aligned} \frac{d\sigma}{d\Omega}(\text{total}) &= \frac{d\sigma}{d\Omega}(\text{elastic}) + \frac{d\sigma}{d\Omega}(\text{charge transfer}) \\ &+ \left[2^3 \sum_{n=2}^{\infty} n^{-3} + \frac{\sigma(\text{total ionization})}{\sigma(\text{total excitation})} \right] \frac{d\sigma}{d\Omega}(\text{excitation, } n=2). \end{aligned} \quad (3)$$

This estimation is shown in Fig. 4 along with the classical calculation. The data in Ref. 1 have been extended by us to larger scattering angles since its publication. This extended data was used for the

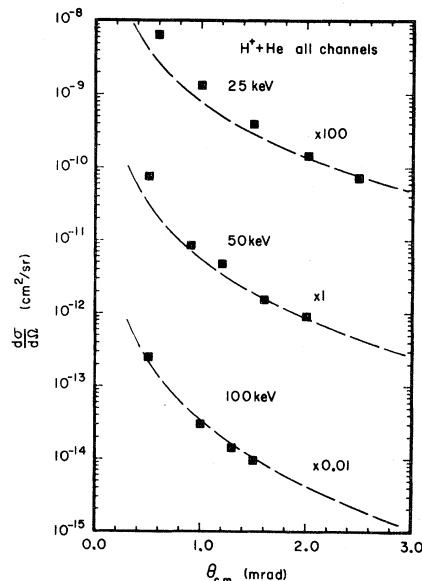


FIG. 4. Estimated total differential cross sections for proton-helium scattering in the center-of-mass frame for a proton with laboratory energies of 25, 50, and 100 keV. ■, estimated total differential cross section; —, classical calculation for elastic differential scattering using the static potential.

also be used to estimate an ionization differential cross section. Both the total ionization cross section and the total excitation cross section increase monotonically with nearly the same slope over this energy range with peak values around 100 keV.^{19,27} If the ionization differential cross section is assumed to have the same angular dependence as the excitation differential cross section, the ionization differential cross section can be estimated as the excitation differential cross section times the ratio of the total ionization cross section to the total excitation cross section. Using the assumptions discussed above the total differential cross section for the proton-helium collision can be estimated as

larger scattering angles. The estimated total differential cross sections are in strikingly good agreement with the classical elastic differential cross section using the static potential.

The results shown in Fig. 4 show that the elastic differential cross section does not dominate the total differential scattering cross section. This can be seen by considering the percent contribution to the total differential cross section according to our estimation. At 25 keV and at 2.5 mrad the contributions to the total differential cross section from the excitation, charge transfer, elastic, and ionization channels are estimated to be about 7, 35, 29, and 29 %, respectively. Likewise at 100 keV and at 1.5 mrad the contributions are estimated to be about 10, 40, 13, and 37 %. At 100 keV the most significant contributions to the total differential cross section are coming from the charge-transfer and ionization channels.

The calculations presented in this paper use the static potential to calculate the elastic differential cross sections. The static potential does not take into account any effect of the other open channels. Likewise the four-state calculation of Flannery and McCann¹⁷ only contains the effect of the $n=2$ -level of helium on the elastic channel which is small. Thus the results of all of the theoretical calculations

presented in this paper are expected to yield a total differential scattering cross section instead of a true elastic differential cross section.

There is obviously room for additional, more sophisticated, theoretical efforts. Additional experimental work extending the range of the scattering angles is also needed. The present effort, however, does provide the first measurement of an elastic differential cross section in the 25–100-keV impact energy range as well as additional information on the importance of the inelastic contributions to the proton-helium differential cross section.

This experiment emphasizes the importance of doing a complete calculation. For elastic scattering no channel can be safely omitted in considering ion-atom scattering in the intermediate energy range.

ACKNOWLEDGMENT

This research was supported in part by the National Science Foundation.

*Current address: LeCroy Research Systems, 700 Main Street, Spring Valley, NY 10977.

†Current address: Texas Instruments Incorporated, P.O. Box 225012, Mail Stop 82, Semiconductor Research Lab, Dallas, TX 75265.

¹J. T. Park, J. M. George, J. L. Peacher, and J. E. Aldag, *Phys. Rev. A* **18**, 48 (1978).

²D. H. Crandall, R. H. McKnight, and D. H. Jaecks, *Phys. Rev. A* **7**, 1261 (1973).

³W. J. Savola, Jr., F. J. Eriksen, and E. Pollack, *Phys. Rev. A* **7**, 932 (1973).

⁴E. W. Thomas, L. A. Leatherwood, and J. E. Harriss, *Phys. Rev. A* **12**, 1835 (1975).

⁵R. L. Fitzwilson and E. W. Thomas, *Rev. Sci. Instrum.* **42**, 1864 (1971).

⁶R. L. Fitzwilson and E. W. Thomas, *Phys. Rev. A* **6**, 1054 (1972).

⁷J. K. Rice and F. W. Bingham, *Phys. Rev. A* **5**, 2134 (1972).

⁸F. W. Bingham, *J. Chem. Phys.* **46**, 2003 (1967).

⁹E. Everhart, G. Stone, and R. J. Carbone, *Phys. Rev.* **99**, 1287 (1955).

¹⁰O. B. Firsov, *Zh. Eksp. Teor. Fiz.* **7**, 308 (1958) [*Sov. Phys.—JETP* **6**, 534 (1958)].

¹¹J. Lindhard, V. Nielsen, and M. Scharff, *K. Dan. Vidensk. Selsk. Mat. Fys. Medd.* **36**, No. 10 (1968).

¹²F. T. Smith, R. P. Marchi, W. Aberth, D. C. Lorentz, and O. Heinz, *Phys. Rev.* **161**, 31 (1967).

¹³F. T. Smith, R. P. Marchi, and K. G. Dedrick, *Phys. Rev.* **150**, 79 (1966).

¹⁴R. P. Marchi and Felix T. Smith, *Phys. Rev.* **139**,

A1025 (1965).

¹⁵I. Amdur and A. L. Smith, *J. Chem. Phys.* **48**, 565 (1968).

¹⁶R. J. Cross, Jr., *J. Chem. Phys.* **48**, 1480 (1968).

¹⁷M. R. Flannery and K. J. McCann, *J. Phys. B* **7**, 1558 (1974).

¹⁸J. T. Park, in *Collision Spectroscopy*, edited by R. G. Cooks (Plenum, New York, 1978).

¹⁹J. T. Park and F. D. Schowengerdt, *Phys. Rev.* **185**, 152 (1969).

²⁰G. W. York, Jr., J. T. Park, J. J. Miskinis, D. H. Crandall, and V. Pol, *Rev. Sci. Instrum.* **43**, 230 (1972).

²¹J. T. Park, *IEEE Trans. Nucl. Sci.* **NS-26**, 1012 (1979).

²²H. L. Cox, Jr. and R. A. Bonham, *J. Chem. Phys.* **47**, 2599 (1967).

²³E. Clementi and C. Roetti, *At. Data Nucl. Data Tables* **14**, 177 (1974); E. Clementi, IBM Research report, 1965 (unpublished).

²⁴See, for instance, L. I. Schiff, *Quantum Mechanics*, 3rd ed. (McGraw-Hill, New York, 1968), pp. 324 and 325 and pp. 339–343.

²⁵P. J. Martin, K. Arnett, D. M. Blankenship, T. J. Kvale, J. L. Peacher, E. Redd, V. C. Sutcliffe, and J. T. Park, *Phys. Rev. A* **23**, 2858 (1981).

²⁶M. R. C. McDowell and J. P. Coleman, *Introduction to the Theory of Ion-Atom Collisions* (North-Holland, Amsterdam, 1970), pp. 321 and 322.

²⁷C. F. Barnett, J. A. Ray, E. Ricci, M. I. Wilkes, E. W. McDaniel, E. W. Thomas, and H. B. Gilbody, *Atomic Data for Controlled Fusion Research* (Oak Ridge National Laboratory, Oak Ridge, 1977), p. A.5.6.